Article citation info:
SAMBORSKI S, WIECZORKIEWICZ J, RUSINEK R. A numerical-experimental study on damaged beams dynamics. Eksploatacja i Niezawodnosc – Maintenance and Reliability 2015; 17 (4): 624–631, http://dx.doi.org/10.17531/ein.2015.4.20.

Sylwester SAMBORSKI
Jakub WIECZORKIEWICZ
Rafal RUSINEK

A NUMERICAL-EXPERIMENTAL STUDY ON DAMAGED BEAMS DYNAMICS

NUMERYCZNO-DOŚWIADCZALNE STUDIUM DYNAMIKI BELEK Z USZKODZENIEM

This paper focuses on analysis of damage influence on dynamical behaviour of beams. Finite Element Method was used to simulate vibrations of beams under three variants of boundary conditions: a cantilever beam, a simply- supported beam and a symmetrically clamped beam. Analysis of natural frequencies of both intact and damaged beams was performed in order to observe the effect of damage on the beams dynamics. Next, recurrence plot technique was applied. Finally, experimental verification is performed to check the numerical results.

***Keywords**: damage detection, recurrence plot, beam dynamics, free vibration.*

W pracy zaprezentowano analizę wpływu uszkodzenia na dynamiczne zachowanie belek. Do symulacji numerycznych użyto Metody Elementów Skończonych gdzie analizowano trzy warianty zamocowania belek: jednostronne utwierdzenie, swobodne podparcie i obustronne utwierdzenie. Przeprowadzono analizę częstości drgań własnych belki nieuszkodzonej i uszkodzonej a następnie zastosowano metodę wykresów rekurencyjnych aby zaobserwować różnice w ich zachowaniu dynamicznym. W ostatnim etapie przeprowadzono weryfikację eksperymentalną uzyskanych wyników symulacji.

***Słowa kluczowe**: detekcja uszkodzeń, wykresy rekurencyjne, dynamika belki, drgania własne.*

1. Introduction

In many contemporary structures various types of defects can appear leading to significant reduction of the element rigidity and changing its overall mechanical behaviour. A special challenge is detection and localization of hidden defects, which can have many forms depending on the scale of the problem, eg. dislocations, voids or inclusions in microscale [43, 49, 44, 3] to macroscopic defects, such as delamination in laminated composites [31] or welds in metallic materials [53, 50]. The current work is focused on testing the applicability of dynamic vibration-based, as well as the space analysis methods to defect detection and localization in 1D (beam) structures. The vibration-based methods have been widely used in the plates and beams dynamics. For example, Manoach et al. [25, 26, 27, 24, 48] analysed the frequencies and modes of free vibrations in order to identify damage in beam and plates. The most interesting aspect of these papers was introduction of the so-called Damage Index exploiting the information given by the Poincaré maps [19]. The authors of the current study aimed at testing other dynamical methods towards detection and localization of defects in structures, which led them to reach for time series analysis.

Experimental time series, especially nonlinear, can be analyzed by means of the method of delay coordinates, which allows to reconstruct a phase space and Poincaré section. This procedure is precisely described in [2, 32] and can be applied for analysis of experimental signals obtained from different kinds of real processes [12, 5] and numerical simulations [40]. For instance, the delay coordinate technique is used for researching dynamics of robot joints [47] and to analyse nonlinear system with dry friction [40]. Interesting contribution in the field of phase space reconstruction is presented in [7, 8, 36] in which the method of delay coordinates is employed for experimental and numerically generated signals, also with noise. Another example can be an impact and a self-excited oscillator with CoulombAmontons friction [13].

On the basis of delay coordinates method, a recurrence plot technique is introduced to analyse linear or non-linear stationary and also non-stationary time series [30]. The formal concept of recurrences was introduced by Henri Poincaré in his seminal work from 1890 [37], for which he won a prize sponsored by King Oscar II of Sweden and Norway [30]. Therein, Poincaré did not only discover the homoclinic tangl which lies at the root of the chaotic behaviour of orbits, but he also introduced (as a by-product) the concept of recurrences in conservative systems. Even though much mathematical work was carried out in the following years, Poincaré's pioneering work and his discovery of recurrence had to wait for more than 70 years for the development of fast and efficient computers to be exploited numerically. The use of powerful computers boosted chaos theory and allowed to study new and exciting systems. Some of the tedious computations needed to use the concept of recurrence for more practical purposes could only be made with this digital tool [30]. In 1987, [5] introduced the method of recurrence plots (RPs) to visualize the recurrences of dynamical systems. Since that time, scientists have been working in various fields have made use of the RPs. Applications of RPs can be found in numerous fields of research such as astrophysics [52], earth sciences [28], engineering [39, 17, 21, 22, 20, 6, 38], biology [11, 23], cardiology, or neuroscience [29, 30, 46, 51], and otolaryngology [41]. Damage detection of various mechanical structure is also analyzed with the help of the RP [34, 35, 42, 33].

Here, in this paper the applicability of the RPs to identify defect in beam structures were tested and compared with the results of different phase space methods; experimental verification of the results was performed, as well.

2. Research methodology

2.1. Numerical model and assumptions

In numerical analyses three variants of boundary conditions (BC) were considered:

- a cantilever beam (Fig.1),
- a simply-supported beam (Fig.2) and
- a beam encastered at both ends (Fig.3).

3. The methodology of analyzing the beams dynamics based on a comparison of the intact and the damaged beam for each of the three BC variants.

The considered numerical beam models prepared in the ABAQUS/CAE software environment had dimensions equal L × B × H = 800 × 20 × 5mm. One of the possibilities of modelling damage in a beam is changing its local stiffness [10, 14]. Thus, both in the FE analyses and in the experimental part of the research a local thinning of the beam was introduced. For the purpose of testing the usefulness of the RPs method in damage identification process the isotropic aluminum beam was tested so far. Nevertheless, the research on the laminated composite beams is in progress. The accepted material data were as follows: mass density ρ=2720kgm−3, Young's modulus E = 70000GPa and Poisson's coefficient ν=0.33. The BCs for the accepted three beam models can formally be written as u(x = 0) = 0, w(x = 0) = 0, dw/dx(x = 0) = 0, u(x = 0) = 0, w(x = 0) = 0, w(x = L) = 0 and u(x = 0) = 0, w(x = 0) =0, dw/dx(x = 0) = 0, u(x = L) = 0, w(x = L) = 0, dw/dx(x = L) = 0.

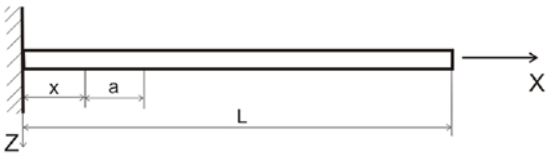

Fig. 1. Cantilever beam model with a defect

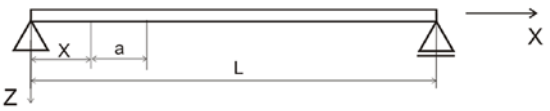

Fig. 2. Simple supported beam model with a defect

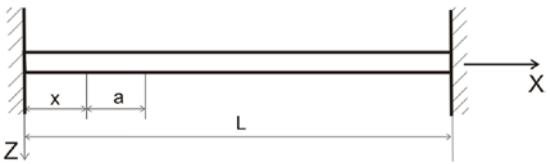

Fig. 3. Clamped-clamped/encastered beam model with a defect

In each case of the BC both damaged and intact beam was analyzed. Such an approach allowed to compare the dynamics of the damaged beams with their undamaged counterparts. In general, for all the models the eigenproblem was solved with the Lanczos algorithm in order to get the frequencies of free vibrations and the respective modes. In the end the elaborated results were collected and compared in order to find the influence of the defect on the dynamical response of the analyzed beam structures. The beam models were composed of the B21 beam-type elements available in the ABAQUS/CAE standard element library [1]. The total number of elements was 40. The defect was modeled as a local thinning of the beam cross-section, as justified above. The weak cross-section had a thickness reduced from the nominal 5mm to 3mm. The defect of the length D=80mm starting at x=40mm from the clamp occupied 10% of the total beam's length. The results obtained with the ABAQUS/CAE were analyzed with the help of different time series analysis and phase space techniques being a background for testing the recurrence plots (RPs) applicability for damage identification. Thus, several scientific approaches were applied simultaneously to find any differences in dynamical output between the intact and the damaged beam.

3.1. Recurrence plots technique

The basic idea of recurrence analysis bases on the delay method where any scalar time series may be used to construct a new time series vector that is equivalent to the original dynamics from a topological point of view. The specific vector in a new space (called the reconstructed space), is formed according to the Takens' theory [45] and can be presented as follows:

$$s_i = (x_i, x_i+d, x_i+_{2d}, \ldots, x_{i+(m-1)d}) \quad (1)$$

where m is called the embedding dimension, d is generally referred as the delay (time delay) or lag. This vector is useful only if parameters m and d are properly chosen. If the delay d is too long, then the coordinates are essentially independent and the proper information cannot be gained from the plot. Whereas the delay d is too short, then the reconstructed states differ not much and the points are scattered around a straight line. The second key embedding parameter m means that we are looking for such dimension of reconstructed phase space to avoid false crossing of the trajectory. If any two points which stay close in the m-dimensional reconstructed space will be still close in the $(m+1)$-dimensional reconstructed space then such a pair of points are called true neighbors, otherwise, they are called false neighbors. One of the most efficient and popular method to choice the time delay d and embedding dimension m are: the average mutual information (AMI) [9] and the false nearest neighbors method (FNN) [18], respectively. In this paper AMI and FNN are used as well.

Recurrence Plot (RP) is an advanced technique of nonlinear data analysis. RP means a visualization of a square matrix, in which the matrix elements correspond to those times at which a state of a dynamical system recurs [30]. The recurrence diagram is expressed by matrix:

$$Ri,j = \mathrm{H}(\varepsilon - |\mathrm{x_i} - \mathrm{x_j}|) \quad (2)$$

where H is the Heaviside step function, ε is a tolerance parameter (threshold),

si and *sj* are a delay vectors (vectors forming the phase space trajectory in the phase space). If the trajectory in the reconstructed phase space returns at time i into the neighbourhood of ε where it was j then M_{ij}=1, other- wise M_{ij}=0. These results are plotted as black and white dots respectively. Detailed description of embedding parameters and much other additional in- formation can be found in [16, 30, 9]. A pattern of RP represents dynamical system behaviour. For instance, periodic motion is reflected by long and non- interrupted diagonals. The vertical distance between these lines corresponds to the period of the oscillation. Irregular motion characterizes the pattern consist of different lengths lines and distance. Here RP technique is used as a method of damage detection in the beams. The embedding parameters: time delay (d) and embedding dimension (m) are estimated first before the recurrence analysis.

3.2. Experimental tests

Experimental verification was performed on the experimental setup presented in Fig.4. The test setup consisted of the Polytec PSV 500

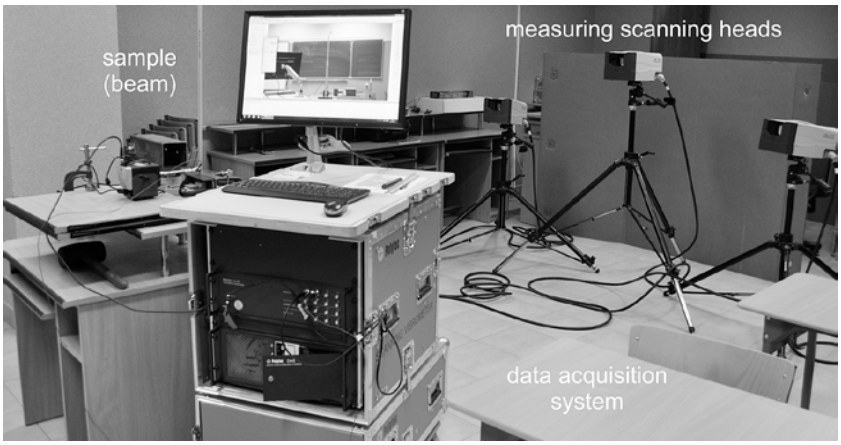

Fig. 4. xperimental standing with 3D Laser Doppler Vibrometer

3D Laser Scanning Vibrometer possessed by Department of Applied Mechanics at Lublin University of Technology.

This sort of vibrometer consists of three in- dependent scanning heads and the data acquisition/visualization unit. Each head is equipped with a laser source; one of them has in addition a video camera. All the three heads have built-in precise transducers able to give dis- placements and velocities of the observed point of the scanned object in time. The three laser beams meet at one point with a defined precision given in microns, what enables highly accurate dynamical measurements, especially around the edges of a specimen. During the measurements a frequency of the laser beam, reflected by the tested object is compared to the one of the sent beam, according to the Doppler effect. Application of the three independent laser scanning heads enables contactless measurements of vibrations of three-dimensional (3D) objects, particularly those having small dimensions. The measurements are simultaneously performed for the three orthogonal spatial directions X, Y and Z. The acquisition/analysis unit is equipped with analog-to-digital data conversion cards. Their task is to collect the measurement data, what is supervised by a dedicated software installed on the PC computer. In addition, the acquisition unit is equipped with an excitation signal generation panel. The laser scanning vibration measurement allows registration of velocities up to 10 m/s in a wide range of frequencies from 0 to 100 kHz. The scanning heads of the PSV500 3D vibrometer enable measurements from 42 cm counting from the object to hundreds of meters [4].

4. Discussion of numerical and experimental results

The first step of the research was the numerical analysis of dynamical behaviour of three beam models differing with boundary conditions (Figs. 1, 2 and 3). Next an experiment was conducted with the Laser Scanning Vibrometer.

4.1. Cantilever beam

The FEA model of the cantilever beam is presented in Fig. 1. In the numerical model the deflection was read at the end point of the beam. The FE simulations gave the eigenfrequencies collected in Tab.1, where the relative differences of the damaged beam's frequencies with respect to the intact one are also presented. In Fig. 5 a direct comparison of free vibration frequencies for both cantilever beams is presented.

Table 1. Eigenfrequencies of the cantilever beam

Eigenfrequency order	Eigenfrequency [Hz]		Relative difference [%]
	intact	damaged	
f_1	6.40	4.43	30.78
f_2	40.11	36.43	9.17
f_3	112.29	108.26	3.59
f_4	219.94	213.44	2.96
f_5	363.36	349.42	3.84

Thus, the reader can see the absolute values of subsequent frequencies; the only slight difference between the frequencies obtained for the damaged beam in comparison with the healthy one is also well seen. Taking into account the frequencies of free vibrations collected in Tab.1 the excitation frequency for the cantilever beam was chosen to be 2 Hz at the sampling frequency of 0.02 s. Such an approach was proposed by Manoach et al. [25, 26, 27]. The load (pressure) was uniformly distributed along the beam. Its value was 1 kPa. The resulting displacement time courses of the beams free end were plotted in Fig. 6. For better visibility of the differences between the damaged and the intact beam a phase plot is shown in Fig. 7. Both the time series and the phase plots show only the difference in vibrations amplitude but the small change in frequency is not observable here. Therefore, the recurrence plot for the delay d=3, embedding dimension m=2 and the neighbourhood ε=0.002 were drawn for the intact and the damaged beam in Fig.8a and b respectively. The former plot obtained for the intact beam (Fig. 8a) pattern characterizes periodic motion. The pattern of the damaged beam (Fig. 8b) reflects also regular vibrations but the amplitude is different from the intact beam output so

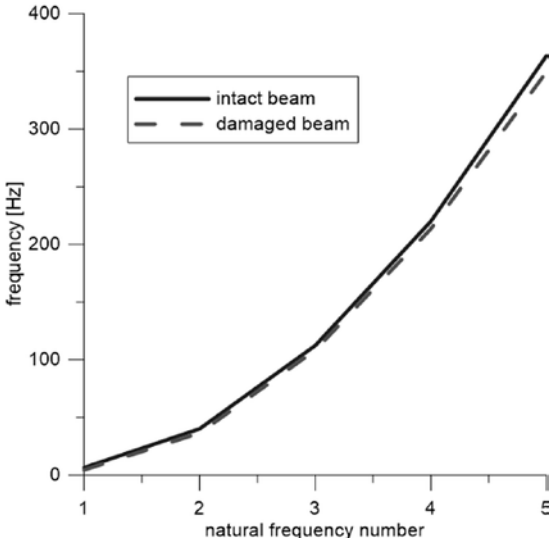

Fig. 5. Comparison of eigenfrequencies for the cantilever intact and damaged beam

it is important to compare both cases in the same neighbourhood size ε.

4.2. Simply supported beam

The simply-supported beam model is presented in Fig. 2. In this case, the displacement (deflection) was measured in the middle of the beam. The eigenfrequencies obtained numerically are given in Tab. 2 and graphically presented in Fig. 9. Again, the frequencies for the intact beam are bigger than those for the damaged beam. Concerning the obtained eigenfrequencies, the excitation frequency was set to 10 Hz, which was in each case less than $f1$, in order to evade the resonance, as the analysis was by assumption linear. For the same reasons the amplitude of the distributed load was set to 10 kPa, what resulted in displacement amplitudes very similar to those obtained for the cantilever beams end; the beam response was sampled every 0.005s.

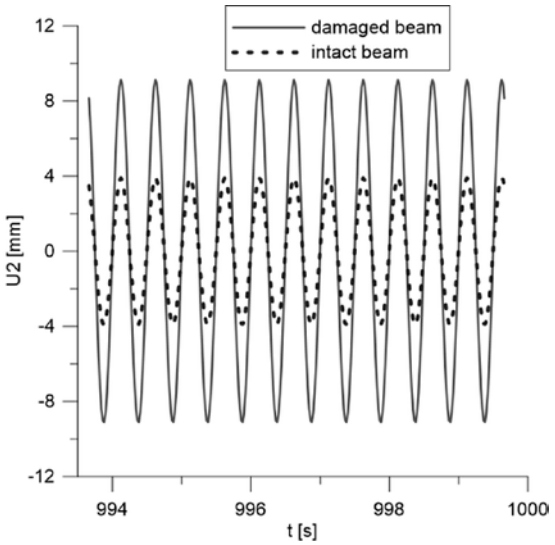

Fig. 6 Displacement time course of intact and damaged cantilever beam forced vibrations at 2Hz

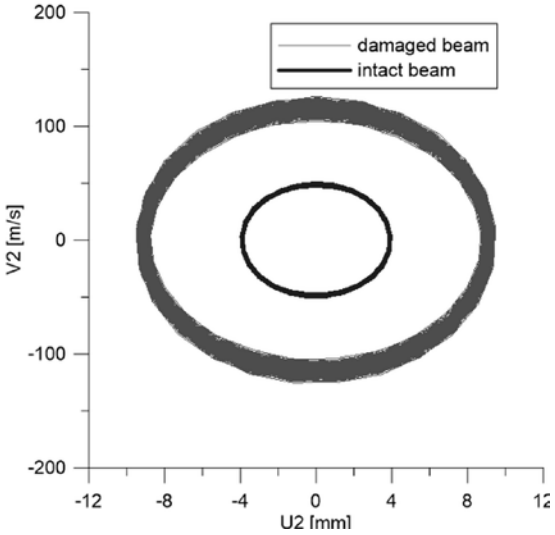

Fig. 7. Phase diagram for the cantilever beam excited at 2 Hz

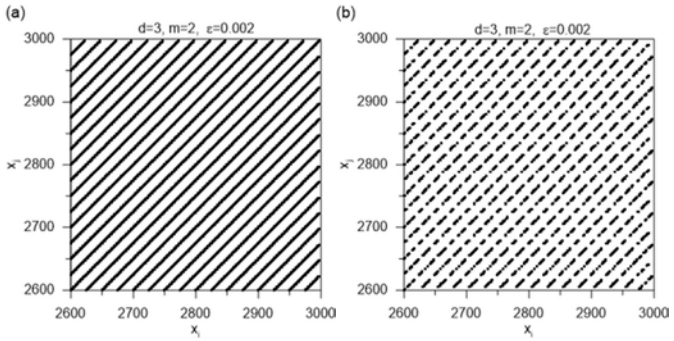

Fig. 8. Recurrence Plot for cantilever intact beam (a) and damaged (b)

The time course (Fig. 10) and the phase plot (Fig. 11) depict the dynamic properties of the simply supported beam. The dynamic behavior of the intact and the damaged structure observed by time series (Fig. 10) and the phase plot (Fig. 11) were very similar to each other but the damaged beam exhibited a bit bigger amplitude of vibrations. The difference between them is more evident in recurrence analysis done for embedding parameters: d=2, m=2 and ε=0.005.

Table 2. Eigenfrequencies of a simply supported beam

Eigenfrequency order	Eigenfrequency [Hz]		Relative difference [%]
	intact	damaged	
f_1	17.97	17.43	3.03
f_2	71.88	65.63	8.70
f_3	161.73	143.71	11.14
f_4	287.49	259.65	9.68
f_5	449.16	416.06	7.37

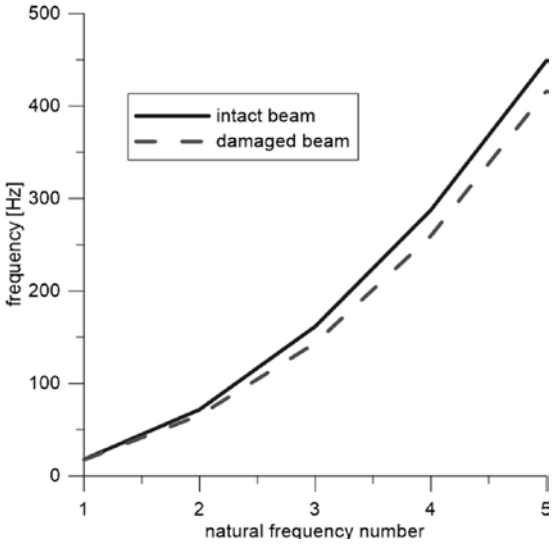

Fig. 9. Comparison of eigenfrequencies for the simply supported intact and damaged beam

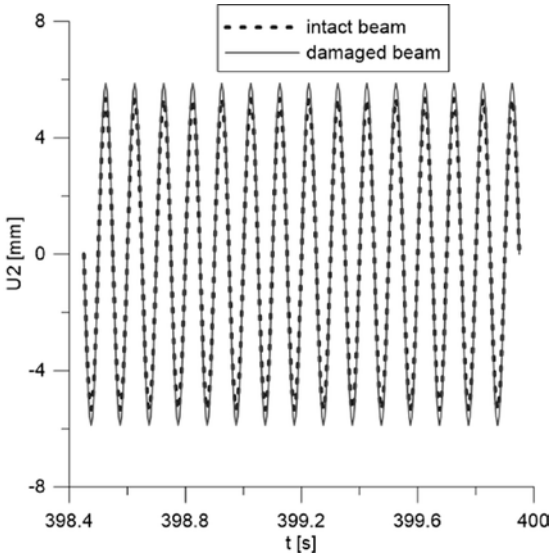

Fig. 10. Displacement time course of intact and damaged simply supported beam forced vibrations at 10Hz

The recurrence plots (Fig. 12) exhibit regular motion of the intact beam while the damaged one manifests a motion with quasi-periodicity that cannot be noticed only through the time series and even the phase plot.

4.3. Clamped-clamped beam

The third model of beam structure was clamped at both ends (Fig. 3). The dimensions of the beam, as well as the size and location of the defect was the same as in the previous two models. However,

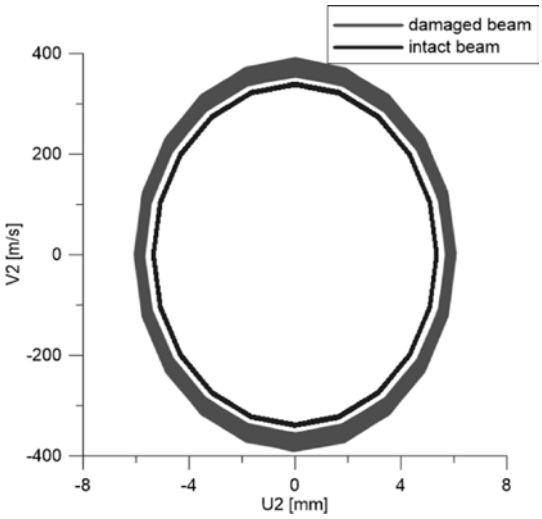

Fig. 11. Phase diagram for the simply supported beam excited at 10 Hz

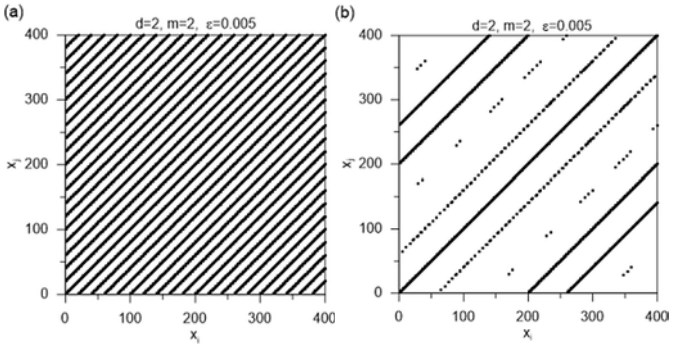

Fig. 12 Recurrence Plot for simply supported intact beam (a) and damaged (b)

Table 3. Eigenfrequencies of the clamped-clamped beam

Eigenfrequency order	Eigenfrequency [Hz]		Relative difference [%]
	intact	damaged	
f_1	40.74	36.82	9.61
f_2	112.30	108.41	3.46
f_3	220.14	213.93	2.82
f_4	363.88	350.43	3.70
f_5	543.52	522.80	3.81

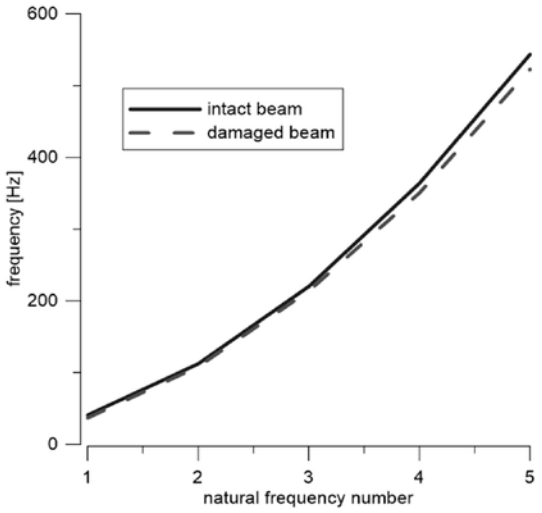

Fig. 13. Comparison of eigenfrequencies for the clamped-clamped intact and damaged beam

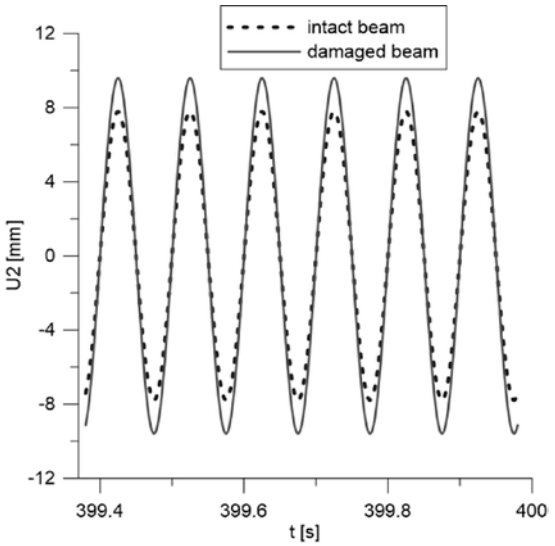

Fig. 14. Displacement time course of intact and damaged clamped-clamped beam forced vibrations at 20 Hz

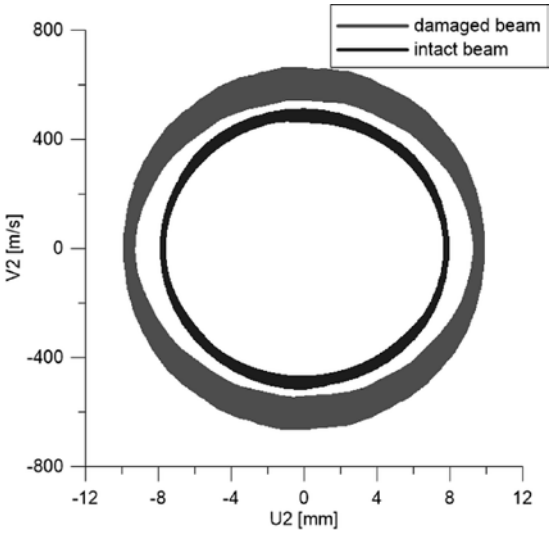

Fig. 15. Phase diagram for the clamped-clamped beam excited at 20Hz

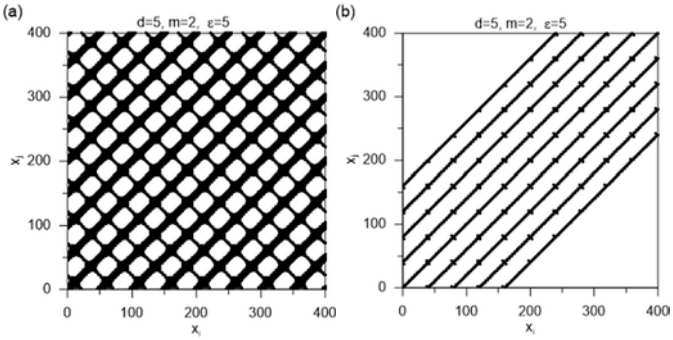

Fig. 16. Recurrence Plot for clamped-clamped intact beam (a) and damaged (b)

for the accepted boundary conditions the beam was much stiffer, what was reflected by its eigenfrequencies collected in Tab.3 and graphically shown in Fig. 13. Also the expected deflections were smaller. For this reason the load amplitude value was chosen to be 1 kPa, what provided approximately the same value of deflection amplitude (measured in the beam's mid-point) compared to the two previous models. The accepted excitation frequency was 20 Hz at 0.005 s sampling. Also in this case the damaged beam was less stiff than the intact one and therefore it had smaller natural frequencies and bigger vibrations

amplitudes, what was reflected by the time series (Fig. 14) and the phase plot (Fig. 15).

The difference in eigenfrequencies was very small specially at first modes that is why simple frequency analysis was not sufficient to detect damages in beams. The recurrence plot technique turned out to give better results provided that embedding parameters are selected properly. Here, for beams clamped at both ends, the embedding parameters were as follows: d=5, m=2 ε=5. Then, the recurrence plots present various pattern depending on the damage existence (Fig. 16). The intact beam (without defect) demonstrates regular RP (Fig. 16a), while irregular pattern is typical for the damaged beam (Fig. 16b). The damaged beam exhibits symptoms of quasi-periodicity.

4.4. Experimental results

The measurements were conducted on a physical aluminum beams, both intact and defected. The BCs provided by the experimental setup in its current form were those given in Fig. 1 – the cantilever beam. The results are collected in Tab. 4. Comparison of the results with those given in Tab. 1 show their good compatibility. Namely, the tendency of subsequent free vibration frequencies for the beam with defect to be smaller than its counterpart obtained for the intact structure was confirmed experimentally. Moreover, the relative differences were the biggest for the first mode, both in simulations and in the experiment. This was of course connected with the applied BCs – clamp at one end. For the higher frequencies the differences were circulating around several percent in both cases. The discrepancies between the numerical results and the experimental ones are now under detailed consideration. The same applies to the experimental setup towards testing the other BCs.

5. Conclusions

Defect detection procedure based on frequency analysis and recurrence plot technique is presented here with quite good results. Since the difference in eigenfrequencies are relatively small especially for lower modes, additional procedure to analyse excited vibrations of identified object is important. The recurrence plots analysis gives a new aspects of the problem. In case of damaged beams recurrence plot pattern is always less regular that let us distinguish intact and damaged structure.

The damaged beams have always bigger amplitude of excited vibrations and smaller natural frequency. That is caused by smaller stiffness of damaged beams comparing to intact beams which do not have any detects. Numerical and experimental results are consistent in this matter.

The difference in the natural frequencies between the intact and damaged beam generally depends on BCs and mode number. Sometimes, it is better to analyse lower modes and sometimes higher ones depending on BCs.

Acknowledgements

Financial support of Structural Funds in the Operational Programme - Innovative Economy (IE OP) financed from the European Regional Development Fund – Project "Modern material technologies in aerospace industry", POIG.01.01.02-00-015/08-00 is gratefully acknowledged.

References

1. Abaqus 6.13: analysis user's manual 2013.
2. Abarbanel HDI Analysis of Observed Chaotic Data. Springer-Verlag, New York 1996.
3. Bathe KJ. Computational fluid and solid mechanics 2003: Proceedings, Second MIT Conference on Computational Fluid and Solid Mechanics, June 17-20, 2003: On the different behaviour of porous ceramic polycrystalline materials under tension and compression stress state, Elsevier, Amsterdam and Boston 2003.
4. Cichon P, Stosiak M. Zastosowanie wibrometru laserowego do pomiaru drgań stołu symulatora liniowego napędu hydrostatycznego. Napędy i Sterowanie 2012; 5: 66–72.
5. Eckmann JP, Kamphorst SO, Ruelle D. Recurrence Plots of Dynamical Systems. Europhysics Letters (EPL) 1987; 4(9): 973–977, http://dx.doi.org/10.1209/0295-5075/4/9/004.
6. Elwakil AS, Soliman AM. Mathematical Models of the Twin-T, Wienbridgeand Family of Minimum Component Electronic Chaos Generators with Demonstrative Recurrence Plots. Chaos, Solitons & Fractals 1999; 10(8): 1399–1412, http://dx.doi.org/10.1016/S0960-0779(98)00109-X.
7. Franca LFP, Savi MA. Distinguishing Periodic and Chaotic Time Series Obtained from an Experimental Nonlinear Pendulum. Nonlinear Dynamics 2001; 26: 253–271, http://dx.doi.org/10.1023/A:1013029607482.
8. Franca LFP, Savi MA. Estimating Attractor Dimension on the Nonlinear Pendulum Time Series. Journal of the Brazilian Society of Mechanical Sciences 2001; 23(4): 427–439, http://dx.doi.org/10.1590/S0100-73862001000400004.
9. Fraser A, Swinney H. Independent coordinates for strange at- tractors from mutual information. Physical Review A 1986; 33(2): 1134–1140, http://dx.doi.org/10.1103/PhysRevA.33.1134.
10. Garc´ıa D, Trendafilova I. A multivariate data analysis approach towards vibration analysis and vibration-based damage assessment. Journal of Sound and Vibration 2014; 333(25): 7036–7050, http://dx.doi.org/10.1016/j.jsv.2014.08.014.
11. Giuliani A, Manetti C. Hidden peculiarities in the potential energy time series of a tripeptide highlighted by a recurrence plot analysis: A molecular dynamics simulation. Physical Review E 1996; 53(6): 6336–6340, http://dx.doi.org/10.1103/PhysRevE.53.6336.
12. Gradisek J, Grabec I, Siegert S, Friedrich R. Stochastic Dynamics of Metal Cutting: Bifurcation Phenomena in Turning. Mechanical Systems and Signal Processing 2002; 16(5): 831–840, http://dx.doi.org/10.1006/mssp.2001.1403.
13. Hinrichs N, Oestreich M, Popp K. Dynamics of Oscillators with Impact and Friction. Chaos Solitons and Fractals 1997; 8(4): 535–558, http://dx.doi.org/10.1016/S0960-0779(96)00121-X.
14. Ismail Z, Kuan KK, Yee KS, Chao OZ. Examining the trend in loss of flexural stiffness of simply supported RC beams with various crack severity using model updating. Measurement 2014; 50: 43–49, http://dx.doi.org/10.1016/j.measurement.2013.12.036.

15. Johnson MA, Moon FC. Nonlinear Techniques to Characterize Prechatter and Chatter Vibrations in the Machining of Metals. International Journal of Bifurcation and Chaos 2001; 2(11): 449–467, http://dx.doi.org/10.1142/S0218127401002171.
16. Kantz H, Schreiber T. Nonlinear Time Series Analysis. Cambridge University Press 1997.
17. Kecik K, Rusinek R, Warminski J. Stability Lobes Analysis of Nickel Superalloys Milling. International Journal of Bifurcation and Chaos 2011; 21(10): 1–12, http://dx.doi.org/10.1142/S0218127411030258.
18. Kennel M, Brown R, Abarbanel H. Determining embedding dimension for phase-space reconstruction using a geometrical construction. Physical Review A 1992; 45(6): 3403–3411.
20. Litak G, Rusinek R Dynamics of a stainless steel turning process by statistical and recurrence analyses. Meccanica 2012; 47(6): 1517–1526, http://dx.doi.org/10.1007/s11012-011-9534-x.
21. Litak G, Kaminski T, Rusinek R, Czarnigowski J, Wendeker M. Patterns in the combustion process in a spark ignition engine. Chaos Solitons and Fractals 2008; 35: 578–585, http://dx.doi.org/10.1016/j.chaos.2006.05.053.
22. Litak G, Syta A, Rusinek R. Dynamical changes during composite milling: recurrence and multiscale entropy analysis. International Journal of Advanced Manufacturing Technology 2011; 56(5-8): 445–453, http://dx.doi.org/10.1007/s00170-011-3195-8.
23. Manetti C, Giuliani A, Ceruso MA, Webber CL, Zbilut JP. Recurrence analysis of hydration effects on nonlinear protein dynamics: multiplicative scaling and additive processes. Physics Letters A 2001; 281(5- 6): 317–323.
24. Manoach E, Trendafilova I. Large amplitude vibrations and dam- age detection of rectangular plates. Journal of Sound and Vibration 2008; 315(3): 591–606, http://dx.doi.org/10.1016/j.jsv.2008.02.016.
25. Manoach E, Samborski S, Mitura A, Warminski J. Vibration based damage detection in composite beams under temperature variations using Poincar´e maps. International Journal of Mechanical Sciences 2012; 62(1): 120–132, http://dx.doi.org/10.1016/j.ijmecsci.2012.06.006.
26. Manoach E, Warminski J, Mitura A, Samborski S. Dynamics of a composite Timoshenko beam with delamination. Mechanics Research Communications 2012; 46: 47–53, http://dx.doi.org/10.1016/j.mechrescom.2012.08.008.
27. Manoach E, Warminski J, Mitura A, Samborski S. Dynamics of a laminated composite beam with delamination and inclusions. The European Physical Journal Special Topics 2013; 222(7): 1649–1664, http://dx.doi.org/10.1140/epjst/e2013-01952-6.
28. Marwan N, Thiel M, Nowaczyk NR. Cross recurrence plot based synchronization of time series. Nonlinear Processes in Geophysics 2002; 9: 325–331, http://dx.doi.org/10.5194/npg-9-325-2002.
29. Marwan N, Wessel N, Meyerfeldt U, Schirdewan A, Kurths J. Recurrence plot-based measures of complexity and their application to heart-rate-variability data. Physical Review E 2002; 66(2), http://dx.doi.org/10.1103/PhysRevE.66.026702.
30. Marwan N, Romano MC, Thiel M, Kurths J. Recurrence plots for the analysis of complex systems. Physics Reports 2007; 438: 237–329, http://dx.doi.org/10.1016/j.physrep.2006.11.001.
31. Muc A, Stawiarski A. Identification of damages in composite multilayered cylindrical panels with delaminations. Composite Structures 2012; 94(5): 1871–1879, http://dx.doi.org/10.1016/j.compstruct.2011.11.026.
32. Nayfeh AH, Balachandran B. Applied Nonlinear Dynamics - Analytical, Computational and Experimental Methods 1995. John Wiley & Sons, Inc., http://dx.doi.org/10.1002/9783527617548.
33. Nichols JM, Trickey ST, Seaver M. Damage detection using multi- variate recurrence quantification analysis. Mechanical Systems and Signal Processing 2006; 20(2): 421–437, http://dx.doi.org/10.1016/j.ymssp.2004.08.007.
34. Nichols JM, Trickey ST, Seaver M, Moniz L. Use of Fiber-optic Strain Sensors and Holder Exponents for Detecting and Localizing Dam- age in an Experimental Plate Structure. Journal of Intelligent Material Systems and Structures 2006; 18(1): 51–67, http://dx.doi.org/10.1177/1045389X06064354.
35. Nomura Y, Morimoto D, Kusaka T, Furuta H. Structural Damage Localization Based on Recurrence Plots of Chaotic Response Attractor. Transactions Of The Japan Society Of Mechanical Engineers Series C 2013; 79(807): 4210–4222, http://dx.doi.org/10.1299/kikaic.79.4210.
36. Piccoli H, Weber H. Experimental Observation of Chaotic Motion in a Rotor with Rubbing. Nonlinear Dynamics 1998; 16: 55–70, http://dx.doi.org/10.1023/A:1008284317724.
37. Poincare H. Introduction. Acta Mathematica 1890; 13(1): 5–7, http://dx.doi.org/10.1007/BF02392506.
38. Rusinek R. Cutting process of composite materials: An experimental study. International Journal of Non-Linear Mechanics 2010; 45: 458–462, http://dx.doi.org/10.1016/j.ijnonlinmec.2010.01.004.
39. Rusinek R. Vibrations In Cutting Process Of Titanium Alloy. Eksploatacja i Niezawodnosc - Maintenance and Reliability 2010; 3: 48–55.
40. Rusinek R, Warminski J. Attractor reconstruction of self-excited mechanical systems. Chaos Solitons and Fractals 2009; 40: 172–182, http://dx.doi.org/10.1016/j.chaos.2007.07.040.
41. Rusinek R, Szymanski M, Warminski J, Zadrozniak M, Morshed K Vibrations in the Human Middle Ear. Medical Science Monitor 2011; 17(12): 372–376, http://dx.doi.org/10.12659/MSM.882123.
42. Sato T, Tanaka Y. Minor Damage Detection Using Chaotic Excitation and Recurrence Analysis. Journal of Earthquake and Tsunami 2011; 05(03): 259–270, http://dx.doi.org/10.1142/S1793431111001054.
43. Sirivedin S, Fenner DN, Nath RB, Galiotis C. Effects of inter- fibre spacing and matrix cracks on stress amplification factors in carbon- fibre/epoxy matrix composites. Part I: planar array of fibres. Composites Part A: Applied Science and Manufacturing 2003; 34(12): 1227–1234, http://dx.doi.org/10.1016/S1359-835X(03)00252-5.
44. Sirivedin S, Fenner DN, Nath RB, Galiotis C. Effects of inter- fibre spacing and matrix cracks on stress amplification factors in carbon-fibre/epoxy matrix composites, Part II: Hexagonal array of fibres. Composites Part A: Applied Science and Manufacturing 2006; 37(11): 1936–1943, http://dx.doi.org/10.1016/j.compositesa.2005.12.022.
45. Takens F. Detecting Strange Attractors in Turbulence. Lecture Notes in Mathematics 1981; 898: 366–381, http://dx.doi.org/10.1007/BFb0091924.
46. Thomasson N, Hoeppner TJ, Webber CL, Zbilut JP. Recurrence quantification in epileptic EEGs. Physics Letters A 2001; 279(1-2): 94–101, http://dx.doi.org/10.1016/S0375-9601(00)00815-X.
47. Trendafilova I, van Brussel H. Non-linear dynamics tools for the motion analysis and condition monitoring of robot joints. Mechanical Systems and Signal Processing 2001; 15(6): 1141–1164, http://dx.doi.org/10.1006/mssp.2000.1394.

48. Trendafilova I, Manoach E. Vibration-based damage detection in plates by using time series analysis. Mechanical Systems and Signal Processing 2008; 22(5): 1092–1106, http://dx.doi.org/10.1016/j.ymssp.2007.11.020.
49. Yu A, Gupta V. Measurement of in situ fiber/matrix interface strength in graphite/epoxy composites. Composites Science and Technology 1998; 58(11): 1827–1837, http://dx.doi.org/10.1016/S0266-3538(98)00048-7.
50. Zahran O, Kasban H, El-Kordy M, El-Samie FA. Automatic weld defect identification from radiographic images. NDT & E International 2013; 57: 26–35, http://dx.doi.org/10.1016/j.ndteint.2012.11.005.
51. Zbilut JP, Koebbe M, Loeb H, Mayer-Kress G. Use of recurrence plots in the analysis of heart beat intervals. In: Computers in Cardiology, 1990: 263–266, http://dx.doi.org/10.1109/CIC.1990.144211.
52. Zolotova NV, Ponyavin DI. Phase asynchrony of the north- south sunspot activity. Astronomy and Astrophysics 2006; 449(1): L1–L4, http://dx.doi.org/10.1051/0004-6361:200600013.
53. Zou Y, Du D, Chang B, Ji L, Pan J. Automatic weld defect detection method based on Kalman filtering for real-time radio- graphic inspection of spiral pipe. NDT & E International 2015; 72: 1–9, http://dx.doi.org/10.1016/j.ndteint.2015.01.002.

Sylwester SAMBORSKI
Jakub WIECZORKIEWICZ
Rafal RUSINEK
Department of Applied Mechanics
Lublin University of Technology
ul. Nadbystrzycka 36, Lublin, 20-618, Poland

E-mail: s.samborski@pollub.pl, j.wieczorkiewicz@pollub.pl, r.rusinek@pollub.pl